CONDENSED
MATTER
PHYSICS

Dynamics of the Rochelle salt NaKC$_4$H$_4$O$_6$·4H$_2$O crystal studied within the Mitsui model extended by piezoelectric interaction and transverse field

R.R. Levitskii[1], A.Ya. Andrusyk[1], I.R. Zachek[2]

[1] Institute for Condensed Matter Physics of the National Academy of Sciences of Ukraine,
1 Svientsitsky Str., 79011 Lviv, Ukraine

[2] Lviv Polytechnic National University, 12 Bandera Str., 79013 Lviv, Ukraine

We calculated dynamic dielectric permittivity of the Rochelle salt within the Mitsui model, extended by piezo-electric interaction and transverse field. Calculations were based on the parameters derived earlier within the study of thermodynamic properties of Rochelle salt. The study of dynamic properties was performed within the Bloch equation method. We showed that taking transverse field into account allows for better description of the Rochelle salt relaxation dynamics. Furthermore, we showed that taking transverse field into account results in the appearance of a resonant component in dynamic permittivity like it is observed in experiment. However, in accordance with the calculations, resonant response reveals itself within infrared frequency range, whereas in experiment it is observed within submillimeter spectral region.

Key words: *Rochelle salt, molecular field approximation, dynamic dielectric permittivity, relaxation dynamics, resonant dynamics*

PACS: *77.22.Ch, 77.80.Bh, 77.84.Fa*

1. Introduction

Ferroelectric crystals of the order-disorder type with asymmetric double-well potential has a number of unusual properties. A good example of such crystal is sodium potassium tartrate tetrahydrate NaKC$_4$H$_4$O$_6$·4H$_2$O (Rochelle salt or Rs). The presence of two Curie points and the existence of the ferroelectric phase within a narrow temperature range (between $T_{c1} = 255$ K and $T_{c2} = 297$ K) is a prominent characteristic of this crystal. Both phase transitions are of the second order [1].

Structural analysis occupies an important place in the study of the Rochelle salt. These studies showed that crystalline structure of Rs proved to be complex. It is orthorhombic (space group $D_2^3 - P2_12_12_1$) in the paraelectric phases and monoclinic (space group $C_2^2 - P2_1$) in the ferroelectric phase [2]. Spontaneous polarization is directed along the a crystal axis; it is accompanied by a spontaneous shear strain ε_4. There are four formula units (112 atoms) in the unit cell of the Rochelle salt. The unit cell is divided into four non-equivalent structural elements, each of which produces a dipole moment both along ferroelectric x- and along y-axes. Consequently, a crystal lattice is divided into four sublattices. Studies based on x-ray diffraction data [3] argued that these were the order-disorder motions of O9 and O10 groups, coupled with the displacive vibrations of O8 groups, which were responsible for the phase transitions in the Rochelle salt as well as for the spontaneous polarization.

Inspite of the achievements in determining the of Rochelle salt structure, the arrangement of hydrogen atoms in the crystal and their role in phase transition still remain unclear. Their important role is testified by significant hydrogen/deuterium isotope effect. Such situation makes *ab-initio* calculations impossible and requires the application of alternative approaches.

We study Rochelle salt properties within the semi-microscopic approach, which is based on the assumption that phase transition in Rochelle salt is of order-disorder type. This assumption

is supported by a system dielectric response of relaxation type, which was derived for microwave region [4–6]. Besides that, neutron diffraction experimental data [7] support the presence of two possible ionic configurations. The dielectric [8], spectroscopic (Raman spectrum) [9] and structural (neutron scattering) [10] studies, carried out in submillimeter range, indicate the presence of resonant response, which is over-damped once one approaches the point of phase transition from low-temperature paraelectric phase, and this is the evidence of phase transition of displacive type.

On the other hand, this resonant response may be caused by dynamic flipping of structural elements between two equilibrium positions. One may expect that the introduction of additional term like transverse field, responsible for dynamic flipping of structural elements, into a model Hamiltonian will permit to make the description of this resonant response. Thus, a simple model like the de Gennes one, can be applicable to the description of Rochelle salt properties.

Mitsui proposed a model of the order-disorder type adequate to Rochelle salt [11]. This model is based on the assumption that structural elements move in asymmetric double well potential and hence have two equilibrium positions. Occupation of one of the equilibrium states results in emergence of a dipole moment. Each cell contains two dipoles. The dipoles form two co-penetrating sublattices with local potentials, which are the mirror reflections of each other. Therefore, even though dipoles in each sublattice are ordered (sublattice polarization is available), the total polarization at certain temperatures may be equal to zero.

The study of the Mitsui model, formulated in terms of pseudospin operators [5, 12], reveals several types of temperature behavior of the model. Depending on the values of model parameters, it can undergo, for instance, a single second order phase transition from ferroelectric into paraelectric phase (observed in RbHSO$_4$), two second order phase transitions (Rs, dRs), one low temperature first order and one high temperature second order phase transition[1] (NH$_4$HSO$_4$), etc. The spontaneous polarization, dielectric permittivity and other thermodynamic characteristics of the crystals mentioned above were calculated and studied within the Mitsui model in the molecular field approximation [12–15].

The relaxation dynamics of the Rs, dRs and RbHSO$_4$ was explored within the Mitsui model too [12, 15–19], where the temperature dependence of relaxation times and dynamic permittivity of these crystals were calculated. Concerning Rochelle salt, it was obtained that relaxation time, exhibiting a critical slowing down at the Curie points, actually diverges at these points. However, experiments [5] indicate that the values of relaxation time are large but remain finite. Moreover, the theoretically calculated and experimental static dielectric permittivities are essentially different: the former diverges at the phase transition points whereas the latter remains finite. Naturally, such inconsistency stems either from the model incompletion or from the defect of the approximation used. Later the Mitsui model was extended by means of the accounting tunnelling effects [12, 16]. Also the Mitsui model was studied within two-particle cluster approximation for the short-range interactions [20]. However, these improvements failed to provide for correct temperature dependence of relaxation time at the phase transition points.

The problem of incorrect temperature dependence of relaxation times and dynamic permittivity for Rs crystal at the Curie points was successfully solved by taking into account piezoelectric interaction of pseudospin subsystem with lattice deformation [21]. Finite relaxation time at the phase transition points was obtained within the extended Mitsui model. This approach allows to experimentally explain the detected difference of the static permittivities of clamped and free crystals. Generally, good agreement of theory and experiment for dielectric permittivities of clamped and free crystals was derived [21]. The unique theory parameter set, providing acceptable agreement of theory and experiment for numerous physical characteristics of the Rochelle salt: elastic, longitudinal dielectric (static and dynamic) and piezoelectric, was first derived in this work.

Recent works deal with new theoretical consideration of the effect produced by external factors like field [22], hydrostatic [23] and uniaxial σ_4 [24] pressures on physical properties of Rs. The effect of partial deuteration on Rochelle salt was studied within the extended Mitsui model [25] as well as piezoelectric resonance in Rs [26]. Taking into consideration a real structure of Rochelle salt crystal, the four-sublattice Mitsui model instead of the two-sublattice Mitsui model was studied [27, 28].

---

[1]Here the additional assumption that the model parameters slightly depend on temperature is needed.

This model explains transverse dielectric properties of Rochelle salt. Also, experiments [29] were carried out for the effect of humidity, annealing, stresses, electric field on dielectric permittivity of Rochelle salt. Modern experimental techniques, applied therein, updated the experimental data, formerly derived for Rs crystal.

Notwithstanding the significant advances in studying the Rs crystal, some problems in theoretically explaining the physical properties of Rochelle salt still remain unsolved. Thus, the theoretically calculated value of spontaneous polarization appeared to be significantly lower than the experimental one along the whole temperature range. Among other things, it has been found that the theoretically calculated real part of dielectric permittivity in low-temperature paraelectric phase is considerably higher than the experimental one. Also, as it was mentioned above, the dielectric response is of resonant type in submillimeter range, and the Mitsui model with piezoelectric interaction is not capable of explaining this fact.

The first problem was successfully solved by taking into account the possibility of dynamic flipping of structural elements between two equilibrium positions [30]. For this purpose Mitsui Hamiltonian with piezoelectric interaction was supplemented with the term of transverse field type. The set of theory model parameters was obtained and on the base thereof some improvement in the description of static dielectric, piezoelectric, and elastic properties was achieved. Besides that, we managed to gradually improve the accordance between theory and experiment for temperature dependence of spontaneous polarization.

In present work we tried to solve two other problems. We carried out our research within Mitsui model with the same consideration of piezoelectric interaction and transverse field. The research was based on the theory parameters derived under consideration of thermodynamics [30]. Besides, we compared our results with the same ones, derived within Mitsui model without transverse field [21], and found out the effect of the transverse field on the dynamic properties of the Rochelle salt.

2. Dynamic physical characteristics of the Mitsui model with piezoelectric interaction and transverse field

We give consideration of the ferroelectric order-disorder type with an asymmetric double-well potential. Hamiltonian of such a system is referred to as the Mitsui Hamiltonian. We assume that this system has an essential piezoelectric interaction which should be taken into account. Besides, the model requires that the transverse field should be taken into account (this term describes the possibility of dynamic ordering units flipping between two equilibrium positions). We suppose the polarization is directed along x-axes and arises due to the structural units ordering in one of the two possible equilibrium positions. We consider the situation when ε_4 component of strain tensor effects the energy of these equilibrium positions. Precisely this case occurs in Rs. The resulting Hamiltonian is of the following form:

$$H = \sum_q \left[\frac{1}{2} v c_{44}^{E0} \varepsilon_4{}^2 - v e_{14}^0 E_{1q} \varepsilon_4 - \frac{1}{2} v \chi_{11}^{\varepsilon 0} E_{1q}^2 \right] - \sum_{q,q'} \left[\frac{J_{qq'}}{2} (S_{q1}^z S_{q'1}^z + S_{q2}^z S_{q'2}^z) + K_{qq'} S_{q1}^z S_{q'2}^z \right]$$
$$- \sum_{qf} \left[\Omega S_{qf}^x + (\Delta_f - 2\psi_4 \varepsilon_4 + \mu E_{1q}) S_{qf}^z \right]. \tag{1}$$

Three terms in the first sum of equation (1) represent the elastic, piezoelectric, and electric energies attributed to a host lattice, in whose potential the pseudospin moves (with the "seed" elastic constant c_{44}^{E0}, the coefficient of piezoelectric stress e_{14}^0, and dielectric susceptibility $\chi_{11}^{\varepsilon 0}$); v is the volume of a cell, containing a pair of pseudospins (ordering units or dipoles) of one lattice site $\mathbf{q}$ and different sublattices $f = 1, 2$ (further we will call it a unit cell[2]). The second sum describes a direct interaction of the ordering units: $J_{qq'} = J_{q'q}$ and $K_{qq'} = K_{q'q}$ are interaction potentials between pseudospins belonging to the same and to different sublattices, respectively. The first term in the third sum is the transverse field; the second term describes a) the energy, associated with

---

[2]Actual unit cell of the Rochelle salt crystal contains two pairs of pseudospins of two lattice sites and different sublattices; therefore, we should set the value of the model unit cell volume to be half of the crystal unit cell volume.

asymmetry of the potential, where Δ_f is asymmetry parameter: $\Delta_1 = -\Delta_2 = \Delta$, b) interaction energy of pseudospin with the field, arising due to the piezoelectric deformation and ψ_4 is the parameter of piezoelectric interaction, c) interaction energy of pseudospin with external electric field E_{1q}, where μ is the effective dipole moment of the model unit cell.

We carry out the study of the system that is described by Hamiltonian (1) within the Bloch equation method. For this purpose we first of all should derive the Hamiltonian within the mean field approximation (MFA).

Performing identical transformation

$$S_{qf}^z = \left\langle S_{qf}^z \right\rangle + \Delta S_{qf}^z \tag{2}$$

and neglecting the quadratic fluctuations, we derive the initial Hamiltonian (1) within MFA:

$$
H_{\mathrm{MFA}} = \sum_q \left[\frac{1}{2} v c_{44}^{E0} {\varepsilon_4}^2 - v e_{14}^0 E_{1q} \varepsilon_4 - \frac{1}{2} v \chi_{11}^{\varepsilon 0} E_{1q}^2 \right]
$$
$$
+ \sum_{qq'} \left[\frac{1}{2} J_{qq'} \left(\left\langle S_{q1}^z \right\rangle \left\langle S_{q'1}^z \right\rangle + \left\langle S_{q2}^z \right\rangle \left\langle S_{q'2}^z \right\rangle \right) + K_{qq'} \left\langle S_{q1}^z \right\rangle \left\langle S_{q'2}^z \right\rangle \right] - \sum_{qf} \boldsymbol{\mathcal{H}}_{qf} \boldsymbol{S}_{qf} \,, \tag{3}
$$

where $\boldsymbol{\mathcal{H}}_{qf}$ are the mean local fields producing the effect on the pseudospins $\boldsymbol{S}_{qf}$:

$$\mathcal{H}_{qf}^x = \Omega, \qquad \mathcal{H}_{qf}^y = 0, \qquad \mathcal{H}_{qf}^z = \varepsilon_{qf} \,,$$

$$\varepsilon_{q1} = \sum_{q'} \left[J_{qq'} \left\langle S_{q'1}^z \right\rangle + K_{qq'} \left\langle S_{q'2}^z \right\rangle \right] + \Delta - 2\psi_4 \varepsilon_4 + \mu E_{1q} \,, \tag{4a}$$

$$\varepsilon_{q2} = \sum_{q'} \left[J_{qq'} \left\langle S_{q'2}^z \right\rangle + K_{qq'} \left\langle S_{q'1}^z \right\rangle \right] - \Delta - 2\psi_4 \varepsilon_4 + \mu E_{1q} \,. \tag{4b}$$

Within MFA we can calculate the mean equilibrium values of the pseudospin operators [30]:

$$\left\langle \boldsymbol{S}_{qf} \right\rangle = \frac{1}{2} \frac{\boldsymbol{\mathcal{H}}_{qf}}{\mathcal{H}_{qf}} \tanh \frac{\mathcal{H}_{qf}}{2k_{\mathrm{B}}T} \,, \tag{5}$$

where $\mathcal{H}_{qf} \equiv |\boldsymbol{\mathcal{H}}_{qf}| = \lambda_{qf}$, and k_{B} is Boltzmann constant.

We study the dynamic properties of the system with Hamiltonian (1) within the Bloch equations method

$$\hbar \frac{\mathrm{d}\left\langle \boldsymbol{S}_{qf} \right\rangle_t}{\mathrm{d}t} = \left\langle \boldsymbol{S}_{qf} \right\rangle_t \times \boldsymbol{\mathcal{H}}_{qf}(t) - \frac{\hbar}{T_1} \left[\left\langle \boldsymbol{S}_{qf} \right\rangle_{t\parallel} - \overline{\left\langle \boldsymbol{S}_{qf} \right\rangle_t} \right] - \frac{\hbar}{T_2} \left\langle \boldsymbol{S}_{qf} \right\rangle_{t\perp} \,. \tag{6}$$

The right hand part of this equation consists of three terms.

The first term is Heisenberg part of the equation of motion, calculated within random phase approximation (RPA), where "×" denotes the vector product and $\boldsymbol{\mathcal{H}}_{qf}(t)$ are the instantaneous values of the local fields[3]:

$$\mathcal{H}_{qf}^x(t) = \Omega, \qquad \mathcal{H}_{qf}^y = 0, \qquad \mathcal{H}_{qf}^z(t) = \varepsilon_{qf}(t), \tag{7}$$

$$\varepsilon_{q1}(t) = \sum_{q'} \left[J_{qq'} \left\langle S_{q'1}^z \right\rangle_t + K_{qq'} \left\langle S_{q'2}^z \right\rangle_t \right] + \Delta - 2\psi_4 \varepsilon_4 + \mu E_{1q}(t), \tag{8a}$$

$$\varepsilon_{q2}(t) = \sum_{q'} \left[J_{qq'} \left\langle S_{q'2}^z \right\rangle_t + K_{qq'} \left\langle S_{q'1}^z \right\rangle_t \right] - \Delta - 2\psi_4 \varepsilon_4 + \mu E_{1q}(t). \tag{8b}$$

---

[3]Original Heisenberg part of the equation of motion is $-\mathrm{i}\langle[\boldsymbol{S}_{qf}, H]\rangle$. Within RPA we calculate the commutator of the pseudospin operators with MFA-Hamiltonian (3). Doing necessary calculations one can derive that

$$-\mathrm{i}\langle[\boldsymbol{S}_{qf}, H]\rangle_t = \left\langle \boldsymbol{S}_{qf} \right\rangle_t \times \boldsymbol{\mathcal{H}}_{qf}(t).$$

We restricted our consideration to sufficiently high frequencies (above the piezoelectric resonance), where the crystal can be regarded to be "clamped" [21]. Mathematically "clamping" means that deformation ε_4 is time independent.

The second and the third terms describe the relaxation of pseudospin towards quasiequilibrium state which is defined by instantaneous values of molecular fields. In particular, the second term describes relaxation of the pseudospin component $\langle \boldsymbol{S}_{qf} \rangle_{t\parallel}$ (longitudinal to the instantaneous value of the local field) towards its quasiequilibrium value with a characteristic time T_1. The third term describes the decay process of the transverse component of pseudospin $\langle \boldsymbol{S}_{qf} \rangle_{t\perp}$ with a characteristic time T_2.

Quasiequilibrium mean values $\overline{\langle \boldsymbol{S}_{qf} \rangle}_t$ are defined as (see equation (5)):

$$\overline{\langle \boldsymbol{S}_{qf} \rangle}_t = \frac{1}{2} \frac{\boldsymbol{\mathcal{H}}_{qf}(t)}{\mathcal{H}_{qf}(t)} \tanh\left(\frac{1}{2}\beta \mathcal{H}_{qf}(t)\right). \tag{9}$$

As we are interested in the linear response of the system to the small external electric field

$$\delta E_{1q}(t), \qquad (E_{1q}(t) = E_1 + \delta E_{1q}(t)),$$

it is sufficient to present $\langle \boldsymbol{S}_{qf} \rangle_t$ as a sum of constant term $\langle \boldsymbol{S}_{qf} \rangle_0$ (mean equilibrium value, calculated in MFA) and time dependent small deviation $\delta \langle \boldsymbol{S}_{qf} \rangle_t$:

$$\langle \boldsymbol{S}_{qf} \rangle_t = \langle \boldsymbol{S}_{qf} \rangle_0 + \delta \langle \boldsymbol{S}_{qf} \rangle_t.$$

Similarly:

$$\boldsymbol{\mathcal{H}}_{qf}(t) = \boldsymbol{\mathcal{H}}_f^{(0)} + \delta \boldsymbol{\mathcal{H}}_{qf}(t), \qquad \overline{\langle \boldsymbol{S}_{qf} \rangle}_t = \langle \boldsymbol{S}_{qf} \rangle_0 + \delta \overline{\langle \boldsymbol{S}_{qf} \rangle}_t.$$

Now, we can linearize the motion equation (6) by retaining the terms, which are linear in deviations $\delta \langle \boldsymbol{S}_{qf} \rangle_t$, $\delta \boldsymbol{\mathcal{H}}_{qf}(t)$, $\delta \overline{\langle \boldsymbol{S}_{qf} \rangle}_t$:

$$\begin{aligned}
\hbar \frac{\mathrm{d}\delta\langle \boldsymbol{S}_{qf} \rangle_t}{\mathrm{d}t} =\ & \delta\langle \boldsymbol{S}_{qf} \rangle_t \times \boldsymbol{\mathcal{H}}_f^{(0)} + \langle \boldsymbol{S}_{qf} \rangle_0 \times \delta\boldsymbol{\mathcal{H}}_{qf}(t) \\
& -\frac{\hbar}{T_1}\Big[\delta\langle \boldsymbol{S}_{qf} \rangle_{t\parallel} - \delta\overline{\langle \boldsymbol{S}_{qf} \rangle}_{t\parallel}\Big] - \frac{\hbar}{T_2}\Big[\delta\langle \boldsymbol{S}_{qf} \rangle_{t\perp} - \delta\overline{\langle \boldsymbol{S}_{qf} \rangle}_{t\perp}\Big],
\end{aligned} \tag{10}$$

where

$$\delta\mathcal{H}_{qf}^x(t) = 0, \qquad \delta\mathcal{H}_{qf}^y(t) = 0,$$

$$\delta\mathcal{H}_{q1}^z(t) = \sum_{q'} J_{qq'}\delta\langle S_{q'1}^z \rangle_t + \sum_{q'} K_{qq'}\delta\langle S_{q'2}^z \rangle_t + \mu\delta E_{1q}(t),$$

$$\delta\mathcal{H}_{q2}^z(t) = \sum_{q'} K_{qq'}\delta\langle S_{q'1}^z \rangle_t + \sum_{q'} J_{qq'}\delta\langle S_{q'2}^z \rangle_t + \mu\delta E_{1q}(t).$$

Now we transform the equation (10) into a form involving single variable $\delta \langle \boldsymbol{S}_{qf} \rangle_t$, then Fourier transform to k-space, introduce new variables

$$\delta \langle \boldsymbol{S}_{k1} \rangle_t = \frac{\delta\boldsymbol{\xi}_k(t) + \delta\boldsymbol{\sigma}_k(t)}{2}, \tag{11a}$$

$$\delta \langle \boldsymbol{S}_{k2} \rangle_t = \frac{\delta\boldsymbol{\xi}_k(t) - \delta\boldsymbol{\sigma}_k(t)}{2}, \tag{11b}$$

and introduce parameters

$$\tilde{R}_k^+ = \frac{\tilde{J}_k + \tilde{K}_k}{2}, \qquad \tilde{R}_k^- = \frac{\tilde{J}_k - \tilde{K}_k}{2},$$

$$\tilde{J}_k = J_k/k_{\mathrm{B}}, \qquad \tilde{K}_k = K_k/k_{\mathrm{B}}. \tag{12}$$

Upon applying these transformations, the Bloch equation (10) is reduced to the system of linear differential equations of the following matrix form:

$$\frac{\hbar}{k_{\mathrm{B}}}\frac{\mathrm{d}x_k(t)}{\mathrm{d}t} = A_k x_k(t) - \tilde{\mu}\delta E_{1k}(t)b, \tag{13}$$

where $\tilde{\mu} = \mu/k_{\mathrm{B}}$,

$$A_k = \begin{pmatrix} a_{11} & a_{12} & -\tilde{\Omega} & 0 & a_{15} & a_{16} \\ a_{21} & a_{22} & 0 & -\tilde{\Omega} & a_{16} & a_{15} \\ a_{31} & a_{32} & -\frac{1}{T_2'} & 0 & a_{35} & a_{36} \\ a_{41} & a_{42} & 0 & -\frac{1}{T_2'} & a_{36} & a_{35} \\ a_{51} & a_{52} & -a_{35} & -a_{36} & a_{55} & a_{56} \\ a_{61} & a_{62} & -a_{36} & -a_{35} & a_{56} & a_{55} \end{pmatrix}, \quad x_k(t) = \begin{pmatrix} \delta\xi_k^z(t) \\ \delta\sigma_k^z(t) \\ \delta\xi_k^y(t) \\ \delta\sigma_k^y(t) \\ \delta\xi_k^x(t) \\ \delta\sigma_k^x(t) \end{pmatrix}, \quad b = \begin{pmatrix} b_1 \\ b_2 \\ \xi^x \\ \sigma^x \\ b_5 \\ b_6 \end{pmatrix}. \tag{14}$$

Components of matrix A_k:

$$a_{11} = -1/T_2' + U_1 + \tilde{R}_k^+(Q_1 + G_1), \quad a_{12} = U_2 + \tilde{R}_k^-(Q_2 + G_2), \quad a_{15} = V_1, \quad a_{16} = V_2,$$
$$a_{21} = U_2 + \tilde{R}_k^+(Q_2 + G_2), \quad a_{22} = -1/T_2' + U_1 + \tilde{R}_k^-(Q_1 + G_1),$$
$$a_{31} = \tilde{\Omega} - \tilde{R}_k^+\xi^x, \quad a_{32} = -\tilde{R}_k^-\sigma^x, \quad a_{35} = -\left[\tilde{R}_0^+\xi^z - 2\tilde{\psi}_4\varepsilon_4\right], \quad a_{36} = -\left[\tilde{R}_0^-\sigma^z + \tilde{\Delta}\right],$$
$$a_{41} = -\tilde{R}_k^+\sigma^x, \quad a_{42} = \tilde{\Omega} - \tilde{R}_k^-\xi^x,$$
$$a_{51} = V_1 + \tilde{R}_k^+H_1, \quad a_{52} = V_2 + \tilde{R}_k^-H_2, \quad a_{55} = -1/T_2' + W_1, \quad a_{56} = W_2,$$
$$a_{61} = V_2 + \tilde{R}_k^+H_2, \quad a_{62} = V_1 + \tilde{R}_k^-H_1; \tag{15}$$

components of vector b:

$$b_1 = -(Q_1 + G_1), \qquad b_2 = -(Q_2 + G_2), \qquad b_5 = -H_1, \qquad b_6 = -H_2, \tag{16}$$

where the following notations are used:

$$Q_{1,2} = \frac{1}{2T_2'}\left(\frac{\xi^z + \sigma^z}{\tilde{\varepsilon}_1} \pm \frac{\xi^z - \sigma^z}{\tilde{\varepsilon}_2}\right), \qquad U_{1,2} = \frac{1}{2}\left(\frac{1}{T_2'} - \frac{1}{T_1'}\right)\left(\frac{\tilde{\varepsilon}_1^2}{\tilde{\lambda}_1^2} \pm \frac{\tilde{\varepsilon}_2^2}{\tilde{\lambda}_2^2}\right),$$

$$V_{1,2} = \frac{1}{2}\left(\frac{1}{T_2'} - \frac{1}{T_1'}\right)\left(\frac{\tilde{\Omega}\tilde{\varepsilon}_1}{\tilde{\lambda}_1^2} \pm \frac{\tilde{\Omega}\tilde{\varepsilon}_2}{\tilde{\lambda}_2^2}\right), \quad W_{1,2} = \frac{1}{2}\left(\frac{1}{T_2'} - \frac{1}{T_1'}\right)\left(\frac{\tilde{\Omega}^2}{\tilde{\lambda}_1^2} \pm \frac{\tilde{\Omega}^2}{\tilde{\lambda}_2^2}\right),$$

$$G_{1,2} = K_1\frac{\tilde{\varepsilon}_1^2}{\tilde{\lambda}_1^2} \pm K_2\frac{\tilde{\varepsilon}_2^2}{\tilde{\lambda}_2^2}, \qquad\qquad H_{1,2} = K_1\frac{\tilde{\Omega}\tilde{\varepsilon}_1}{\tilde{\lambda}_1^2} \pm K_2\frac{\tilde{\Omega}\tilde{\varepsilon}_2}{\tilde{\lambda}_2^2},$$

$$K_{1,2} = \frac{1}{T_1'}\frac{1}{4T\left(\cosh\frac{\tilde{\lambda}_{1,2}}{2T}\right)^2} - \frac{1}{2T_2'}\frac{\xi^z \pm \sigma^z}{\tilde{\varepsilon}_{1,2}},$$

$$\tilde{\Omega} = \frac{\Omega}{k_{\mathrm{B}}}, \qquad \tilde{\Delta} = \frac{\Delta}{k_{\mathrm{B}}}, \qquad \tilde{\psi}_4 = \frac{\psi_4}{k_{\mathrm{B}}}, \qquad \tilde{\varepsilon}_{1,2} = \frac{\varepsilon_{1,2}}{k_{\mathrm{B}}}, \qquad \tilde{\lambda}_{1,2} = \frac{\lambda_{1,2}}{k_{\mathrm{B}}}. \tag{17}$$

Relaxation times T_1' and T_2' have the following form:

$$T_1' = \frac{k_{\mathrm{B}}}{\hbar}T_1, \qquad T_2' = \frac{k_{\mathrm{B}}}{\hbar}T_2. \tag{18}$$

After applying the time Fourier transformation we transform equation (13) to the form

$$\left(A_k - \mathrm{i}\frac{\hbar}{k_{\mathrm{B}}}\omega I\right)x_k(\omega) = \tilde{\mu}\delta E_{1k}(\omega)b, \tag{19}$$

where I is identity matrix. It is convenient to present the solution of equation (19) in the form

$$x_k(\omega) = \tilde{\mu}\delta E_{1k}(\omega)\left[\left(A_k - \mathrm{i}\frac{\hbar}{k_{\mathrm{B}}}\omega I\right)^{-1}b\right], \tag{20}$$

where we denote the inverse matrix of $\left(A_k - i\frac{\hbar}{k_B}\omega I\right)$ by $\left(A_k - i\frac{\hbar}{k_B}\omega I\right)^{-1}$.

Expression for fluctuation of polarization

$$\delta P_{1k}(\omega) = \chi_{11}^{\varepsilon 0}(\mathbf{k})E_{1k} + \frac{\tilde{\mu}}{\tilde{v}}\delta\xi_k^z(\omega)$$

and solution (20) allows us to come up with the final expression for permittivity:

$$\varepsilon_{11}(\mathbf{k},\omega) = \varepsilon_{11}(\mathbf{k},\infty) + 4\pi\frac{\tilde{\mu}^2}{\tilde{v}}F_1(\mathbf{k},i\omega), \tag{21}$$

$$F_1(\mathbf{k},i\omega) = \left[\left(A_k - i\frac{\hbar}{k_B}\omega I\right)^{-1}b\right]_1, \tag{22}$$

where $\varepsilon_{11}(\mathbf{k},\infty) = 1 + 4\pi\chi_{11}^{\varepsilon 0}(\mathbf{k})$ is a high frequency contribution into the dielectric permittivity and $\tilde{v} = v/k_B$. If $\mathbf{k} = 0$ we have $\varepsilon_{11}(\mathbf{0},\infty) \equiv \varepsilon_{11}(\infty)$ and $\varepsilon_{11}(\infty) = 1 + 4\pi\chi_{11}^{\varepsilon 0}$, where $\chi_{11}^{\varepsilon 0}$ is a "seed" dielectric susceptibility. Index "1" on the right side of equation (22) means the first component of the vector derived by multiplying matrix $\left(A_k - i\frac{\hbar}{k_B}\omega I\right)^{-1}$ and vector b (index "1" arises from the fact that $\delta\xi_k^z(\omega)$ is the first component of vector $x_k(\omega)$).

The analysis shows that susceptibility $\varepsilon_{11}(\mathbf{0},0)$, obtained according to equation (21) equals the static susceptibility obtained earlier for the Mitsui model with piezoelectric interaction and transverse field at $\mathbf{k} = 0$, $\omega = 0$, and at any relaxation times T_1 and T_2. If we set the transverse field equal to zero and identify T_1 with parameter α, which is a characteristic time of the pseudospins chaning their states within Glauber approach, we derive the dynamic permittivity which strictly corresponds to the one derived earlier [21].

It can be easily seen that the function $F_1(\mathbf{k},i\omega)$ is a rational function of $i\omega$, where numerator is a polynomial function of the degree not higher than 5 and denominator is polynomial function of the degree 6. Therefore, we can decompose the function $F_1(\mathbf{k},i\omega)$ into partial fractions:

$$F_1(\mathbf{k},i\omega) = \sum_{i=1}^{n}\frac{k_i\tau_i}{1 + i\omega\tau_i} + \sum_{j=1}^{m}\frac{M_j(i\omega) + N_j}{(i\omega)^2 + p_j(i\omega) + q_j}. \tag{23}$$

Here coefficients k_i, τ_i, M_j, N_j, p_j, q_j are real numbers, n is the number of real (equal to $-1/\tau_i$) eigenvalues and $2m$ is the number of complex eigenvalues of matrix A_k. The number of real and the number of complex eigenvalues of matrix A_k is defined by theory parameters and temperature. However, it is clear that matrix A_k has 6 eigenvalues in total. The first sum in equation (23) is a contribution of Debye (relaxation) modes into the dynamic dielectric permittivity, and the second sum is a contribution of resonant modes.

In paraelectric phase the dynamic dielectric permittivity is as follows:

$$\varepsilon_{11}^{(0)}(\mathbf{k},\omega) = \varepsilon_{11}(\mathbf{k},\infty) + 4\pi\frac{\tilde{\mu}^2}{\tilde{v}}F_1^{(0)}(\mathbf{k},i\omega), \tag{24}$$

$$F_1^{(0)}(\mathbf{k},i\omega) = \left[\left(A_k^{(0)} - i\frac{\hbar}{k_B}\omega I\right)^{-1}b^{(0)}\right]_1. \tag{25}$$

Here matrix $A_k^{(0)}$ and vector $b^{(0)}$ are as follows[4]:

$$A_k^{(0)} = \begin{pmatrix} a_{11} & -\tilde{\Omega} & a_{16} \\ a_{31} & -\frac{1}{T_2'} & -\tilde{\varepsilon} \\ a_{61} & \tilde{\varepsilon} & a_{55} \end{pmatrix}, \quad b^{(0)} = \begin{pmatrix} b_1 \\ b_3 \\ b_6 \end{pmatrix}, \tag{26}$$

---

[4]In paraelectric phase we have $\xi^z = 0$ and $\sigma^x = 0$. Accordingly, matrix A_k in paraelectric phase has two invariant subspaces of dimension 3 and fluctuations $\delta\xi_k^z(\omega)$ are defined by matrix $A_k^{(0)}$ which produces the effect only on one of the subspaces.

where

$$a_{11} = -1/T_2' + U + \tilde{R}_k^+(Q+G), \qquad a_{31} = \tilde{\Omega} - \tilde{R}_k^+ \xi^x,$$
$$a_{16} = V, \qquad a_{61} = V + \tilde{R}_k^+ H, \qquad a_{55} = -1/T_2' + W; \qquad (27)$$

vector $b^{(0)}$ components:

$$b_1 = -(Q+G), \qquad b_3 = \xi^x, \qquad b_6 = -H, \qquad (28)$$

and the following notations are used:

$$Q = \frac{1}{T_2'}\frac{\sigma^z}{\tilde{\varepsilon}}, \qquad U = \left(\frac{1}{T_2'} - \frac{1}{T_1'}\right)\frac{\tilde{\varepsilon}^2}{\tilde{\lambda}^2}, \qquad V = \left(\frac{1}{T_2'} - \frac{1}{T_1'}\right)\frac{\tilde{\Omega}\tilde{\varepsilon}}{\tilde{\lambda}^2},$$

$$W = \left(\frac{1}{T_2'} - \frac{1}{T_1'}\right)\frac{\tilde{\Omega}^2}{\tilde{\lambda}^2}, \qquad G = 2K\frac{\tilde{\varepsilon}^2}{\tilde{\lambda}^2}, \qquad H = 2K\frac{\tilde{\Omega}\tilde{\varepsilon}}{\tilde{\lambda}^2},$$

$$K = \frac{1}{T_1'}\frac{1}{4T\left(\cosh\frac{\tilde{\lambda}}{2T}\right)^2} - \frac{1}{2T_2'}\frac{\sigma^z}{\tilde{\varepsilon}}, \qquad \tilde{\lambda} = \sqrt{\tilde{\Omega}^2 + \tilde{\varepsilon}^2}, \qquad \tilde{\varepsilon} = \tilde{R}_0^- \sigma^z + \tilde{\Delta}. \qquad (29)$$

Hence, depending on the eigenvalues of matrix $A_k^{(0)}$, the dynamics in paraelectric phase is described either by three relaxation modes or one relaxation and one resonant mode.

Žekš [16] obtained the expression for relaxation time in paraelectric phase within the Mitsui model with transverse field, though without piezoelectric interaction. The study was carried out within Bloch equation method at $1/T_2 = 0$. The linear dependence of relaxation time on longitudinal one-particle relaxation time T_1 was derived. However, linear dependence is valid only for large T_1 and is not valid in general case. Besides, the expression for relaxation time of [16] contains an error. In the Appendix we present the correct results for the relaxation time.

In the present work all calculations were carried out in the center of the Brillouin zone $\mathbf{k} = 0$ and in the absence of external electric field $E_1 = 0$.

3. Discussion

We need theory model parameters for particular calculations. We will use a model parameter set derived earlier under consideration of the Rochelle salt thermodynamic properties [30]. These parameters and parameters derived within the analogous model without transverse field [21] are presented in table 1.

In order to calculate dynamic characteristics it is necessary to determine longitudinal and transverse relaxation time T_1, T_2. The results of research show that the alteration of time T_2 within interval $(0.1T_1, \infty)$ has hardly any effect upon the calculated dynamic characteristics; this is illustrated in figure 1.

Weak dependence of the dielectric permittivity allows us to set $T_2 = \infty$ in our calculations. Thus, we completely neglect the decay of transverse component of pseudospin caused by external factors (e.g. interaction with thermostat). However, in this case the decay of transverse component along the whole temperature range occurs anyway (all poles of function $F_1(\mathbf{0}, \mathrm{i}\omega)$ have a negative real part). But now it is caused exceptionally by the internal dynamics of the system and by the relaxation of longitudinal component of pseudospin towards its quasiequilibrium value.

The value of parameter T_1

$$T_1 = 1.767 \times 10^{-13}\ \mathrm{s}$$

was derived based on the agreement between theory and experimental data [5] for ε'_{11} in the upper phase transition point at $\nu = 2.5$ GHz: $\varepsilon'_{11} = 164.53$. For comparison, the value of parameter α, which defines the time scale in Glauber model and which was obtained based on the same condition is equal to 1.7×10^{-13} s [21].

First, we shall present the structure of theoretically derived dynamic response of the Rs. The structure of the dynamic dielectric permittivity is defined by poles of function $F_1(\mathbf{0}, \mathrm{i}\omega)$. This

Table 1. Optimal values of theory parameters for Rochelle salt. Two parameters sets for the models with and without transverse field are presented.

	$\tilde{\Omega} = 0.0$ K	$\tilde{\Omega} = 113.467$ K
$\tilde{J}_0$ (K)	797.36	813.216
$\tilde{K}_0$ (K)	1468.83	1447.17
$\tilde{\Delta}$ (K)	737.33	719.937
$\tilde{\psi}_4$ (K)	−760.0	−720.0
c_{44}^{E0} (10^{10} N/m^2)	1.28	1.224
e_{14}^0 (10^{-2} C/m^2)	3.336	31.64
$\chi_{11}^{\varepsilon 0}$	0.318	0.0
$\mu(T) = a + k(T - 297)$		
a (10^{-30} Cm)	8.41	8.157
k (10^{-30} Cm/K)	−0.022	−0.0185
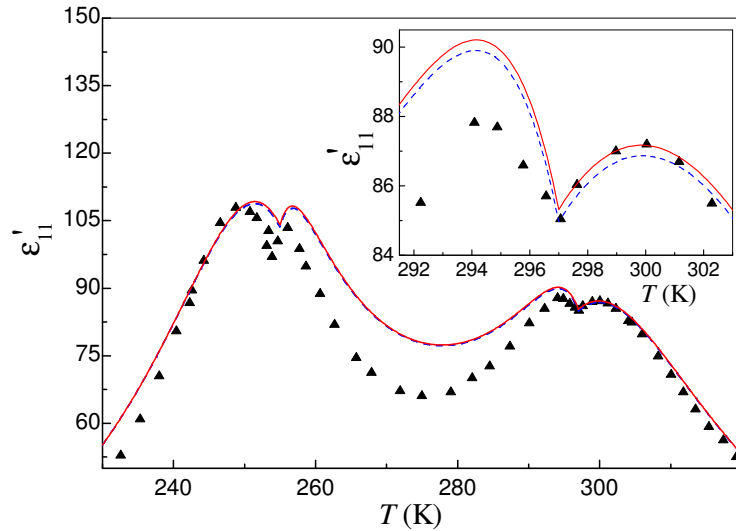
Figure 1. Dependence of a real part of dielectric permittivity on temperature at frequency of $\nu = 5.1$ GHz. Solid line represents calculations at $T_1 = 1.767 \times 10^{-13}$ s, $T_2 = \infty$. Dashed line represents calculations at $T_1 = 1.767 \times 10^{-13}$ s, $T_2 = 0.1T_1$. Dots represent experimental data [5].

function has two real negative poles throughout the whole temperature interval, which determine the two relaxation modes. Besides, this function has two pairs of complex conjugate poles with a negative real part. Each pair of complex conjugate poles determines a resonant mode. However, in the paraelectric phase, one relaxation and one resonant mode give zero contribution into the dielectric permittivity. Hence, in ferroelectric phase dielectric permittivity has the form:

$$\varepsilon_{11}(\omega) = \varepsilon_{11}(\infty) + \frac{k_1'\tau_1}{1 + i\omega\tau_1} + \frac{k_2'\tau_2}{1 + i\omega\tau_2} + \frac{M_1'(i\omega) + N_1'}{(i\omega)^2 + p_1(i\omega) + q_1} + \frac{M_2'(i\omega) + N_2'}{(i\omega)^2 + p_2(i\omega) + q_2},$$

and in paraelectric phases, the dielectric permittivity is as follows:

$$\varepsilon_{11}^{(0)}(\omega) = \varepsilon_{11}(\infty) + \frac{k_1'\tau_1}{1 + i\omega\tau_1} + \frac{M_1'(i\omega) + N_1'}{(i\omega)^2 + p_1(i\omega) + q_1}.$$

Primed and non-primed values differ by the factor of $4\pi\tilde{\mu}^2/\tilde{v}$ (see equations (21) and (23)). Such a characteristic of dielectric response also remains unchanged in the case with finite T_2. Within the model without a transverse field, the dynamics is determined by only two relaxation modes. Both modes have non-zero contribution within ferroelectric phase and only one of them has non-zero contribution within paraelectric phase [21].

Temperature dependencies of two relaxation times τ_1, τ_2, obtained here, along with the same ones derived within the model without transverse field [21] and data for relaxation time obtained on the basis of analysis of experiment for $\varepsilon'_{11}(\nu, T)$ are presented in figure 2. As this figure illustrates,
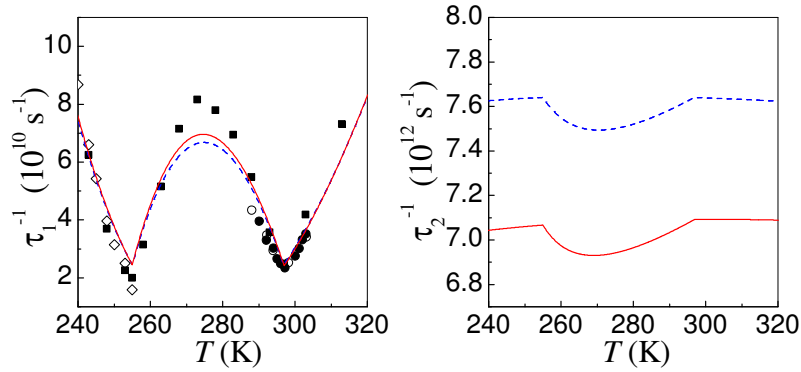
Figure 2. Dependency of inverse relaxation times on temperature. Solid line corresponds to the model with transverse field, dashed line corresponds to the model without transverse field [21]. Points correspond to experimental data: ● ([4]), ■ ([5]), ○ ([6]), ◇ ([31]).
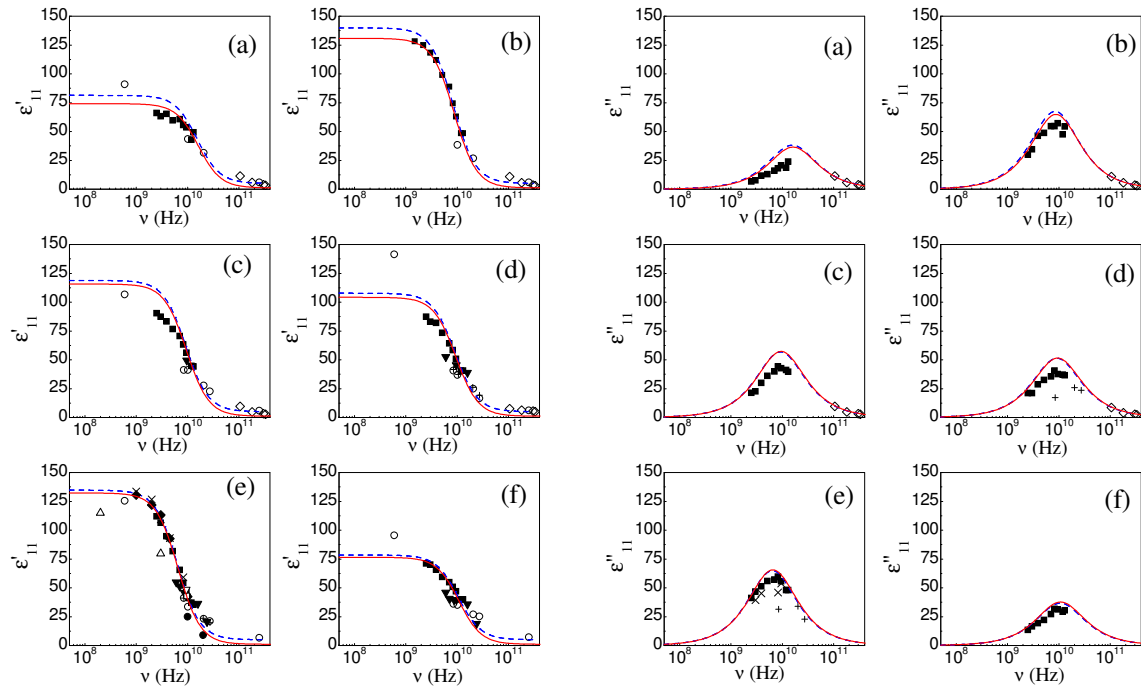
Figure 3. The frequency dependence of the real and imaginary part of dielectric permittivity, calculated within the model with transverse field (solid line) and without transverse field (dashed line [21]) at different temperatures T (K): (a) 235, (b) 245, (c) 265, (d) 285, (e) 305, (f) 315. Points represent experimental data: ■ ([5]), ○ ([32 and 33]), + ([34]), ▼ ([35]), ● ([36]), ♦ ([4]), × ([6]), ◇ ([31]), △ ([37]), ▽ ([38]).

the model with transverse field ensures a better agreement of the theory with the experiment in comparison with the model without transverse field.

Figure 3 presents frequency dependencies of dielectric permittivity in dispersion region ($10^9 - 10^{11}$ Hz) calculated within the models with transverse field and without it at different temperatures along with experimental data. As figures show, both models ensure good agreement between theory and experiment. However, the model with transverse field provides for better agreement of theory with experiment at $T = 235$ K, $T = 245$ K (low temperature paraelectric phase). At other temperatures the agreement between the results, obtained for both models and experimental data are about the same.

The analysis shows that the contribution of the first relaxation mode consists of more than 99% of the total permittivity along the whole temperature range. Thus, the dynamics of Rs within microwave region is of Debye relaxation type. The same conclusion was derived within the model without transverse field [21].
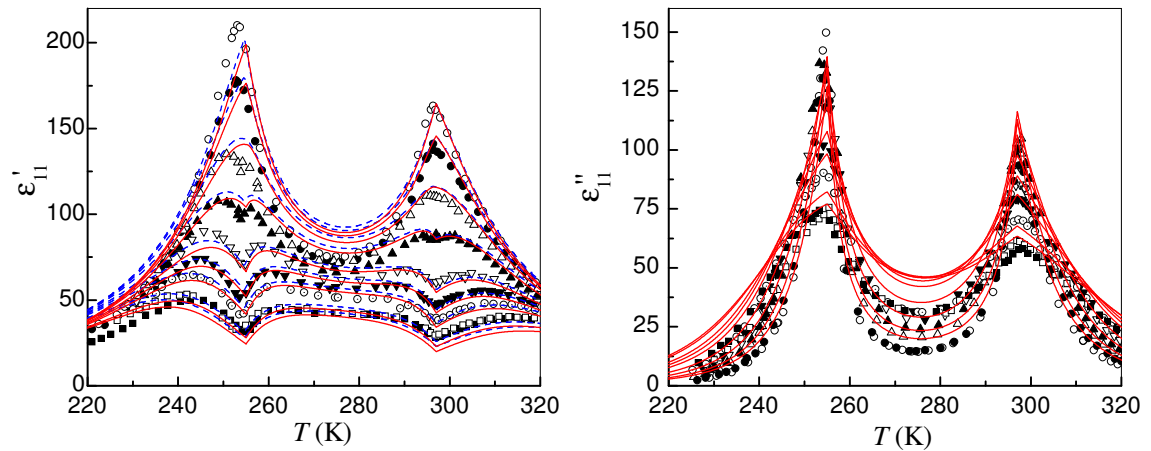

Figure 4. Temperature dependencies of the real and imaginary part of dielectric permittivity at different frequencies. Points represent the results of measurements [5] at frequencies (GHz): ○ 2.5, ● 3, △ 3.9, ▲ 5.1, ▽ 7.05, ▼ 8.25, ⊙ 9.45, □ 11.96, ■ 12.95. Lines represent the results of theoretical calculations carried out within the model with transverse field (solid line) and without transverse field (dashed line [21]) at frequencies corresponding to experiment.

Figures 4, 5 illustrate temperature dependencies of dielectric permittivity ε_{11}, calculated at different frequencies, together with experimental data. Solid and dashed lines present results of calculations derived within (this work) and without (results of work [21]) transverse field respectively. In figure 4 we do not present an imagined part of dielectric permittivity, calculated within the model without transverse field. However, it should be noted that in this case both models provide for about the same agreement of theory with experiment. As figure 4 shows, the model with transverse field provides for better agreement between theory and experiment for a real part of dielectric permittivity. It should also be pointed out that transverse field being taken into account to some extent rectifies the problem of poor agreement between theory and experiment in a low temperature paraelectric phase. Besides, if we assume that a real effective dipole moment has a weaker dependence on temperature (lower in a lower phase transition point and higher in an upper phase transition point), it becomes clear (see equation (24)) that we will reach a better agreement between theory and experiment for a real part of this characteristic in low temperature paraelectric phase. Earlier [30] it was mentioned that such an assumption may allow us to reach a better agreement between theory and experiment for polarization and static dielectric permittivity of a free crystal in a low temperature paraelectric phase.

Now, we calculate the temperature dependence of dielectric permittivity within a wide frequency range and try to find out whether our model with transverse field is capable of describing the resonant dynamics. Figure 6 shows both the experimental data and theoretical calculations for
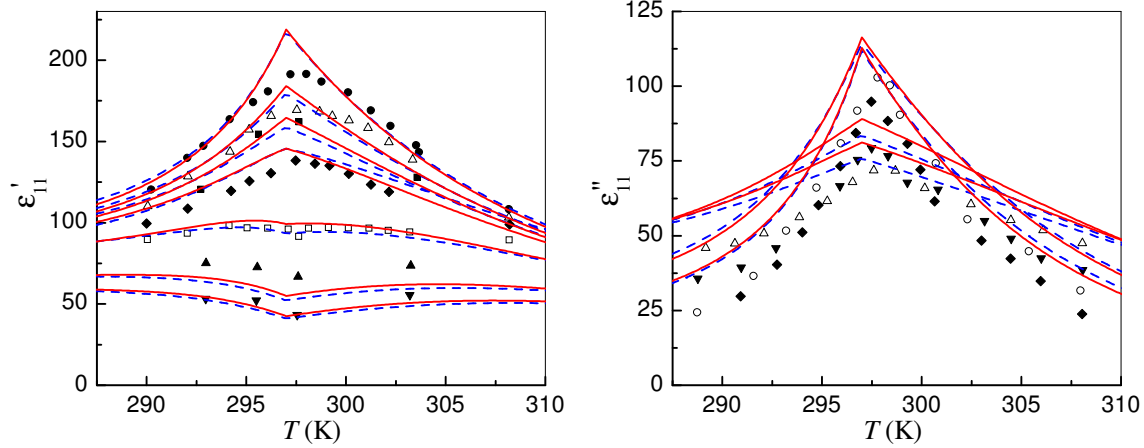
Figure 5. The temperature dependence of the real and imaginary parts of the dynamic dielectric permittivity at different frequencies. Points represent experiment [6] at frequencies (GHz): • 1, △ 2, ■ 2.5, ◇ 3, □ 4.5, ▲ 7, ▼ 8.25. Lines represent the results of theoretical calculations carried out within the model with transverse field (solid line) and without transverse field (dashed line [21]) at frequencies corresponding to experiment.
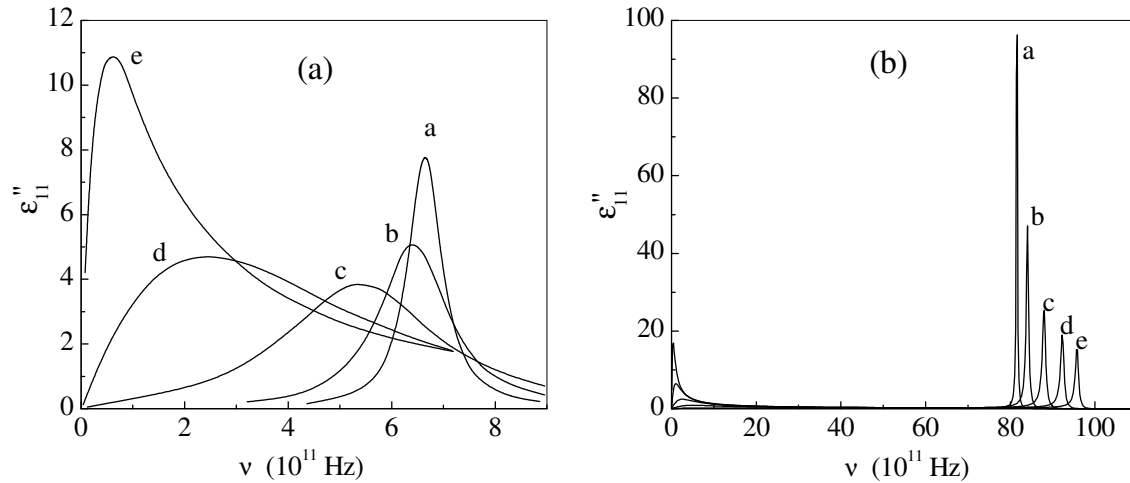

Figure 6. The frequency dependence of the imaginary part of the dynamic dielectric permittivity at different temperatures (K): a – 80, b – 114, c – 150, d – 187, e – 218. Experimental data (a) of [8] and results of theoretical calculations (b) are presented.

frequency dependence of imaginary part of the dielectric permittivity. As one can see, the model with transverse field has a resonant dielectric response at frequency $\nu = 8 \times 10^{12}$ Hz ($T = 80$ K), while the experiment shows a resonant peak at frequency $\nu = 6.6 \times 10^{11}$ Hz. Besides, the theoretically calculated changes of the dielectric spectra with the temperature increase, differ from the corresponding experimental data.

4. Concluding remarks

In this work we studied the dynamic properties of the Rochelle salt. We used the Mitsui model with piezoelectric interaction extended by transverse field. Such an extension allows us to take into account the dynamic flipping of the structural ordering units between two equilibrium positions. The study was performed within the Bloch equation method.

Parameters, required for calculations, were taken from the study of the thermodynamic char-

acteristics (static dielectric, elastic and piezoelectric) [30], where good agreement between theory and experiment was achieved. Two additional parameters (single-particle relaxation times T_1 and T_2) which characterize dynamic processes were defined in the present work. In particular, it was obtained that throughout the whole temperature range the change of T_2 has a little effect on dielectric permittivity in dispersion range and it can be selected as needed for calculation convenience. By appropriate selection of the parameter T_1 we managed to achieve a better agreement between theory and experiment for dynamic dielectric permittivity in comparison with the model that does not take transverse field into account. Therefore, within the Mitsui model with piezoelectric interaction and transverse field, the unique parameter set was derived that well describes both thermodynamic and dynamic properties of the Rochelle salt.

In addition, in this work we revealed the presence of the resonant response within certain frequency range along with relaxation dynamics within microwave range. However, while experiment shows resonant response on frequencies close to $6 \cdot 10^{11}$ Hz, the theory shows resonant response on frequencies $8 \cdot 10^{12} - 10 \cdot 10^{12}$ Hz. The character of changes of dielectric spectrum at temperature increase is essentially different from the experimental data. Currently we have no explanation to such discrepancy. One can notice that our approach has a free parameter T_2. But the variation of this parameter did not permit us to reach an acceptable agreement between theory and experiment for resonant dynamics. Hence, one can conclude that modification of the Mitsui model by taking the transverse field into account is not sufficient in order to properly explain the resonant dielectric response. The additional degrees of freedom are probably essential in resonant response.

Acknowledgements

Appendix. Relaxation time in paraelectric phase calculated within the Mitsui model with transverse field

Here we study the dependence of the relaxation time on the theory model parameter T_1 in paraelectric phase ($\xi^z = 0$, $\sigma^x = 0$). We consider the model with transverse field but neglect transverse relaxation of the pseudospin ($1/T_2 = 0$). Analogous model, but without piezoelectric interaction was considered earlier [16]. It should be noted that in paraelectric phase, piezoelectric interaction just effects the value of σ^z but does not change the analytic formula for the relaxation time.

Relaxation time is defined as

$$\tau = -\hbar/(k_{\mathrm{B}}\Lambda), \tag{30}$$

where Λ is a real eigenvalue of the matrix $A_k^{(0)}$. In our case this matrix has the following form:

$$A_k^{(0)} = \begin{pmatrix} -\dfrac{\tilde{\varepsilon}^2 \varkappa_k}{T_1' \tilde{\lambda}^2} & -\tilde{\Omega} & -\dfrac{\tilde{\Omega}\tilde{\varepsilon}}{T_1' \tilde{\lambda}^2} \\ \tilde{\Omega}\beta_k & 0 & -\tilde{\varepsilon} \\ -\dfrac{\tilde{\Omega}\tilde{\varepsilon}\varkappa_k}{T_1' \tilde{\lambda}^2} & \tilde{\varepsilon} & -\dfrac{\tilde{\Omega}^2}{T_1' \tilde{\lambda}^2} \end{pmatrix}, \tag{31}$$

where the following notations are used:

$$\varkappa_k = 1 - \frac{\tilde{R}_k^+}{2T\left(\cosh\frac{\tilde{\lambda}}{2T}\right)^2}, \qquad \beta_k = 1 - \frac{\tilde{R}_k^+}{\lambda}\tanh\frac{\tilde{\lambda}}{2T}, \qquad \tilde{\lambda} = \sqrt{\tilde{\Omega}^2 + \tilde{\varepsilon}^2}, \qquad \tilde{\varepsilon} = \tilde{R}_0^- \sigma^z + \tilde{\Delta}.$$

All eigenvalues of the matrix $A_k^{(0)}$ are roots of the following characteristic polynomial:

$$W(x) = x^3 + \frac{1}{T_1'}a_1 x^2 + a_2 x + \frac{1}{T_1'}a_3, \tag{32}$$

where constants a_1, a_2, a_3 are independent of T_1' and have the following form:

$$a_1 = \frac{\tilde{\Omega}^2 + \tilde{\varepsilon}^2 \varkappa_k}{\tilde{\lambda}^2}, \qquad a_2 = \tilde{\varepsilon}^2 + \tilde{\Omega}^2 \beta_k, \qquad a_3 = \tilde{\Omega}^2 \beta_k + \tilde{\varepsilon}^2 \varkappa_k.$$

Let us assume that a real root of polynomial $W(x)$ at large T_1' is proportional to $1/T_1'$:

$$\Lambda = z/T_1'. \tag{33}$$

Then we can present $W(x)$ in the following form:

$$W(x) = (x - z/T_1')(x^2 + b_1(T_1')x + b_2) \tag{34}$$

where the constant z is independent of T_1' and $b_1(T_1')$ is an unknown function of T_1'. Expanding last presentation of $W(x)$ one can derive that

$$W(x) = x^3 + \left(b_1(T_1') - \frac{z}{T_1'}\right)x^2 + \left(b_2 - \frac{b_1(T_1')}{T_1'}\right)x - \frac{1}{T_1'}zb_2. \tag{35}$$

Comparing the last terms of equation (32) and equation (35) one can conclude that

$$-zb_2 = a_3 \tag{36}$$

and hence b_2 is independent of T_1'.

Comparing the coefficients near x^2 of polynomial $W(x)$ presented in forms (32) and (35) one can derive the following result for $b_1(T_1')$:

$$b_1(T_1') = \frac{a_1 + z}{T_1'}. \tag{37}$$

Now comparing the corresponding coefficients of $W(x)$ near x and taking into account equation (37) one can derive that

$$b_2 = a_2 + \frac{a_1 + z}{T_1'^2}. \tag{38}$$

Here the last term is a higher-order term that can be neglected. Hence, we can put

$$b_2 = a_2. \tag{39}$$

According to equations (36), (39) one can derive the constant z:

$$z = -\frac{a_3}{a_2}. \tag{40}$$

According to equations (30), (33), and equation (40) the relaxation time at large T_1 is presented as:

$$\tau = T_1 \frac{1 + \varphi}{1 + \varphi\left(1 - \frac{\tilde{R}_k^+}{2T\left(\cosh\frac{\tilde{\lambda}}{2T}\right)^2}\right)}, \tag{41}$$

where

$$\varphi = \frac{\tilde{\varepsilon}^2}{\tilde{\Omega}^2\left(1 - \frac{\tilde{R}_k^+}{\tilde{\lambda}}\tanh\frac{\tilde{\lambda}}{2T}\right)}. \tag{42}$$

Figure 7 presents the results of calculations of the dependence τ on T_1 at $T = 240$ K and $\mathbf{k} = 0$. Both the results of direct calculations (relaxation time derived through numerical finding of the real eigenvalue of the matrix $A_k^{(0)}$) and the results derived based on equation (41) are presented. As one can see, the result of direct calculations rapidly approaches the asymptote. When $T_1 = 1.767 \times 10^{-13}$ s, approximation (41) almost perfectly agrees with the relaxation time calculated directly. This result is valid for the whole paraelectric temperature range.
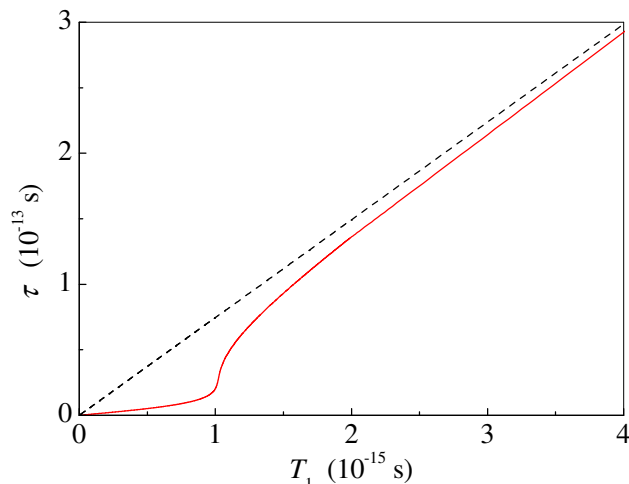
Figure 7. Dependence of the relaxation time on the model parameter T_1 calculated at $T = 240$ K. Solid line presents the results of 'direct' calculations. Dashed line presents the results of calculations based on (41).

References

1. Jona F., Shirane G., Ferroelectric Crystals. Pergamon Press Inc., Oxford, 1962.
2. Solans X., Gonzalez-Silgo C., Ruiz-Pérez C., J. Solid State Chem., 1997, **131**, 350.
3. Kulda J., Hlinka J., Kamba S., Petzelt J., ILL: Annual Report, 2000 [www.ill.fr/AR-00/p-48.htm].
4. Müser H.E., Pottharst J., Phys. Status Solidi, 1967, **109**.
5. Sandy F., Jones R.V., Phys. Rev., 1968, **168**, 481.
6. Kolodziej H. – In: Dielectric and Related Molecular Processes, Vol. 2. The Chemical Society Burlington House, London, 1975, p. 249–287.
7. Iwata Y., Mitani S., Shibuya O., Ferroelectrics, 1990, **107**, 287.
8. Volkov A.A., Goncharov Yu.G., Kozlov G.V., Kryukova Ye.B., Petzelt J., Pis'ma Zh. Éksp. Teor. Fiz., 1985, **41**, 16 [JETP Lett., 1985, **41**, 17].
9. Kamba S., Schaack G., Petzelt J., Phys. Rev. B, 1995, **51**, 14998.
10. Hlinka J., Kulda J., Kamba S., Petzelt J., Phys. Rev. B, 2001, **63**, 052102.
11. Mitsui T., Phys. Rev., 1958, **111**, 1529.
12. Žekš B., Shukla G.G., Blinc R., Phys. Rev. B, 1971, **3**, 2306.
13. Vaks V.G., Introduction into Microscopic Theory of Ferroelectrics. Nauka, Moscow, 1973 (in Russian).
14. Kalenik J., Acta Phys. Pol., 1975, **A48**, 387.
15. Mori K., Ferroelectrics, 1981, **31**, 173.
16. Žekš B., Shukla G.G., Blinc R., J. Phys. Colloq., Suppl., 1972, **33**, C2.
17. Levitskii R.R., Zachek I.R., Varanitskii V.I., Ukr. Fiz. Zh., 1980, **25**, 1766 (in Russian).
18. Levitskii R.R., Zachek I.R., Varanitskii V.I., Fiz. Tverd. Tela (Leningrad), 1980, **22**, 2750 [Sov. Phys. Solid State, 1980, **22**, 1603].
19. Levitskii R.R., Antonyak Yu.T., Zachek I.R., Ukr. Fiz. Zh., 1981, **26**, 1835 (in Russian).
20. Levitskii R.R., Sokolovskii R.O., Condens. Matter Phys., 1999, **2**, 393.
21. Levitskii R.R., Zachek I.R., Verkholyak T.M., Moina A.P., Phys. Rev. B, 2003, **67**, 174112.
22. Moina A.P., Slivka A.G., Kedyulich V.M., Phys. Stat. Sol. B, 2007, **244**, 2641.
23. Levitskii R.R., Moina A.P., Andrusyk A.Ya., Slivka A.G., Kedyulich V.M., J. Phys. Stud., 2008, **11**, 2603.
24. Levitskii R.R., Zachek I.R., Moina A.P., Verkholyak T.M., J. Phys. Stud., 2003, **7**, 106.
25. Levitskii R.R., Zachek I.R., Moina A.P., Andrusyk A.Ya., Condens. Matter Phys., 2004, **7**, 111.
26. Moina A.P., Levitskii R.R., Zachek I.R., Phys. Rev. B, 2005, **71**, 134108.
27. Stasyuk I.V., Velychko O.V., Ferroelectrics, 2005, **316**, 51.
28. Levitskii R.R., Zachek I.R., Vdovych A.S., Stasyuk I.V., Condens. Matter Phys., 2009, **12**, 295.
29. Slivka A.G., Kedyulich V.M., Levitskii R.R., Moina A.P., Romanyuk M.O., Guivan A.M., Condens. Matter Phys., 2005, **8**, 623.

30. Levitskii R.R., Zachek I.R., Andrusyk A.Ya. (unpublished)
31. Volkov A.A., Kozlov G.V., Lebedev S.P., Zh. Eksp. Teor. Fiz., 1980, **79**, 1430 [Sov. Phys. JETP, 1980, **52**, 722].
32. Poplavko Yu.M., Meriakri V.V., Pereverzeva L.P., Alesheckin V.V., Molchanov V.I., Fiz. Tverd. Tela (Leningrad), 1974, **15**, 2515 [Sov. Phys. Solid State, 1974, **15**, 1672].
33. Poplavko Yu.M., Solomonova L.P., Bull. Acad. Sci. USSR, Phys. Ser. (Engl. Transl.), 1967, 1771.
34. Pereverzeva L.P. – In: Mechanisms of Relaxation Phenomena in Solids. Kaunas, 1974 (in Russian).
35. Deyda H., Z. Naturforschg, 1967, **22a**, 1139.
36. Akao H., Sasaki T., J. Chem. Phys., 1955, **23**, 2210.
37. Petrov V.M., Sov. Phys. Crystallogr., 1962, **7**, 403.
38. Jäckle W., Z. Angew. Phys., 1960, **12**, 148.

Дослідження динамічних властивостей сегнетової солі NaKC$_4$H$_4$O$_6$·4H$_2$O в рамках моделі Міцуї, що враховує п'єзоелектричну взаємодію та поперечне поле

Р.Р. Левицький[1], А.Я. Андрусик[1], І.Р. Зачек[2]

[1] Інститут Фізики Конденсованих Систем НАН України, 79011 Львів, вул. Свєнціцького, 1, Україна
[2] Національний Університет "Львівська Політехніка", 79013 Львів, вул. Бандери, 12, Україна

В рамках моделі Міцуї, що враховує п'єзоелектричну взаємодію та поперечне поле розраховано динамічну діелектричну проникність сегнетової солі. Розрахунки проведено на основі параметрів теорії, одержаних раніше при дослідженні термодинамічних властивостей сегнетової солі. Дослідження проведено в рамках методу рівнянь Блоха. Показано, що розширення моделі Міцуї врахуванням поперечного поля та п'єзоелектричної взаємодії дозволяє краще описати релаксаційну динаміку сегнетової солі. Крім того показано, що врахування поперечного поля у моделі Міцуї приводить до появи резонансної складової у динамічній проникності так, як це спостерігається експериментально. Проте згідно проведених розрахунків резонансний відгук проявляє себе у інфрачервоному частотному діапазоні, тоді як на експерименті він спостерігається у субміліметровому діапазоні.

Ключові слова: *сегнетова сіль, наближення молекулярного поля, динамічна діелектрична проникність, релаксаційна динаміка, резонансна динаміка*